Journal of MATERIALS RESEARCH

Invited Feature Paper
DOI: 10.1557/jmr.2020.54

EARLY CAREER SCHOLARS IN MATERIALS SCIENCE

ANNUAL ISSUE

Prediction of relative globularization rates in α + β titanium alloys as a function of initial crystal orientation

Benjamin A. Begley[1], Keith Markham[2], Michael Mizak[2], Adam L. Pilchak[3], Victoria M. Miller[1,a)]

[1]Department of Materials Science and Engineering, University of Florida, Gainesville, Florida 32611, USA
[2]Department of Materials Science and Engineering, North Carolina State University, Raleigh, North Carolina 27695, USA
[3]Air Force Research Laboratory, Materials and Manufacturing Directorate, Wright-Patterson AFB, Ohio 45433, USA
[a)]Address all correspondence to this author. e-mail: victoria.miller@ufl.edu
This paper has been selected as an Invited Feature Paper.
Received: 23 October 2019; accepted: 19 February 2020

The breakdown of the columnar grains and lamellar α + β colony microstructure in two-phase Ti alloys during conversion of ingot to billet is critical to the development of desired combination of mechanical properties. Colony breakdown occurs during a series of thermomechanical processing steps in the α + β phase field. However, fundamental knowledge of the microstructural dependence of this transformation is limited, particularly its dependence on the initial orientation of the α + β colony relative to the imposed strain-path. In this study, the viscoplastic self-consistent polycrystal plasticity model is used to examine deformation behavior as a function of crystal loading direction. Criteria were developed to predict relative globularization rates; it was found that both slip system activities in the α phase and relative crystal rotations of each phase must be considered. Predictions are demonstrated to be consistent with literature and suggest that further experimental investigation of relative globularization rates is necessary.

Victoria M. Miller

Assistant Professor Victoria (Tori) Miller has been in the Department of Materials Science and Engineering at University of Florida since September 2019. She received her B.S.E. in Materials Science and Engineering from the University of Michigan in 2011 and completed her Ph.D. in the Materials Department at the University of California Santa Barbara in 2016. After graduate school, she worked for a year at UES, Inc. as a Research Scientist onsite in the Materials and Manufacturing Directorate of the Air Force Research Laboratory in Dayton, OH. She had also previously worked at Ford Motor Company Research and Development, Toyota Engineering and Manufacturing North America, and Lockheed Martin Aeronautics. Miller's interests include defect and structural evolution in crystalline material and experimental characterization via advanced electron microscopy techniques. She is particularly focused on deformation processing of metals and the associated microstructural evolution, particularly texture evolution, recovery, and recrystallization. Her group's primary focus is on linking macroscopic processing phenomena to micro- and nanoscale mechanisms, enabling the development of predictive material models for engineering applications. Much of the group's work has been in thermomechanical processing of low-symmetry metals including titanium alloys for aerospace and magnesium alloys for automotive and consumer electronic applications.

Introduction

Near-α and α + β titanium alloys are used for flight-critical rotating hardware in the fan and compressor section of gas turbine engines. To develop the appropriate balance of mechanical properties, these alloys are subjected to a complex, multistep thermomechanical processing route. A typical sequence to convert an ingot to billet involves one or more homogenization steps and a series of hot working steps both above and below the β transus. An allotropic phase transformation, β → α + β, occurs each time the material is cooled from above the β transus and vice versa [1].

Because of the limited thermal conductivity of titanium and the volume of material during the large-scale intermediate stages of conversion, large colonies of aligned α platelets form in Burgers orientation relationship (BOR) with the parent β phase [2]. The BOR aligns $(0001)\|\{110\}$ and $\langle 11\bar{2}0\rangle\|\langle 111\rangle$ [3].

It is desirable to refine the large colonies by α + β hot working because the lamellar microstructure resulting from the allotropic transformation has low strength, limited ductility, and poor fatigue resistance [4]. The dynamic and static processes for spheroidization of α laths have been studied extensively [5, 6, 7, 8, 9, 10]. The primary mechanism begins with dynamic formation of subgrain boundaries across the alpha laths that increase in misorientation with increasing strain [11]. The spheroidization process proceeds statically through subsequent heat treatment, activating diffusional processes like thermal grooving to balance interfacial energies [5, 12] and termination end migration [13, 14]. By comparison, behavior of the β phase has received considerably less attention, and it is generally assumed that the β phase must also be recrystallized during the spheroidization process.

However, some reconstructions of transformed β packets in bimodal microstructures [4, 15] have revealed that packets of adjacent transformed β may have low misorientation over long ranges of microstructure. To be consistent with the prevalent terminology in the titanium literature, we hereafter refer to the long–range correlation of beta phase orientations as "β microtexture."

The origins of β microtexture can be traced back to an intermediate mill processing step in which the material is β annealed and quenched for the last time before all subsequent working is performed in the two-phase field. During this step, the prior β grain size is set and large colonies in BOR with the parent β phase are formed during cooling. During the remaining α + β hot working steps, three possibilities for microstructure evolution may be encountered:

(i) *Antirotation:* Burger-related colonies in unstable orientations with respect to the imposed deformation may rotate in different directions, resulting in high misorientation from the initial BOR.
(ii) *Corotation:* Colonies in unstable orientations may rotate cooperatively toward a stable end configuration, maintaining the BOR.
(iii) *Stable Orientations:* Colonies in stable orientations will not undergo significant rotation and the BOR will survive.

We hypothesize that β microtexture may persist through large strain deformation under the second condition, with corotation of both phases that maintains the BOR, and also under the third condition, with minimal rotation of both phases. Under these assumptions, there should exist some ranges of orientation space that favor the breakdown of lamellar colonies and others ranges where breakdown is not favorable. If this is the case, the colony orientations for a given loading direction that correspond to each of these conditions can be predicted through simple plastic rotation arguments. In this work, this hypothesis is tested using the viscoplastic self consistent (VPSC) polycrystal plasticity model.

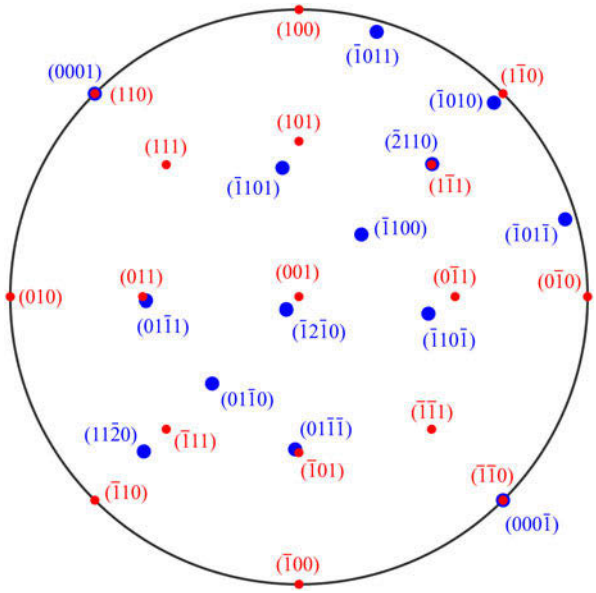

Figure 1: Initial α (blue) + β (red) colony orientation, plotted on an upper hemisphere equal angle projection. All of the included spherical projection plots are relative to this orientation relationship.

Results and discussion

The initial colony orientation is illustrated in Fig. 1. All spherical projection plots presented as part of this work are equal angle projections plotted in reference to this initial orientation. The blue (α phase) and red (β phase) coloring is used throughout this work. More than 900 uniaxial compression directions were simulated as described in the Methods section, uniformly sampling one hemisphere of orientation space to take advantage of the loading symmetry associated with uniaxial tests. Deformation was carried out to a compressive strain of 1.0.

At each VPSC deformation step, the angular deviation from the original ideal BOR was calculated for each loading direction. Animated GIFs of the evolution of this misorientation angle over the full range of strains are presented in the Supplementary material, Fig. S1. The misorientation angles at the final strain of 1.0 are presented in Fig. 2(a). Interestingly, the VPSC results for some orientations predict that the maximum misorientation occurs at an intermediate deformation step instead of at the final strain. The maximum misorientation predicted for each loading direction is plotted in Fig. 2(b). An animated GIF showing the maximum misorientation evolving with strain is presented in the Supplementary material Fig. S2. In these plots, high misorientation angles correspond to the antirotation condition and would be predicted to result in more rapid globularization. Low

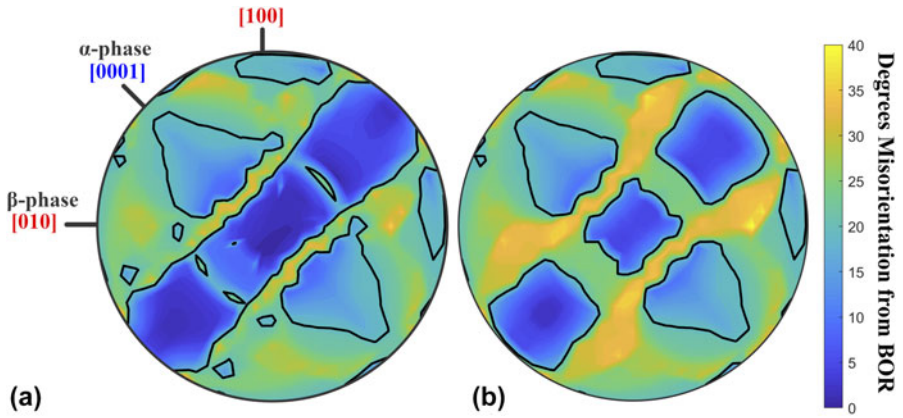

Figure 2: Maximum misorientation from the initial BOR (a) at the final strain of 1.0 and (b) reached at any strain during deformation. A black contour line indicates a misorientation of 20° from BOR. The indicated crystallographic directions in this and future plots show the α and β phase orientations as demonstrated in Fig. 1.

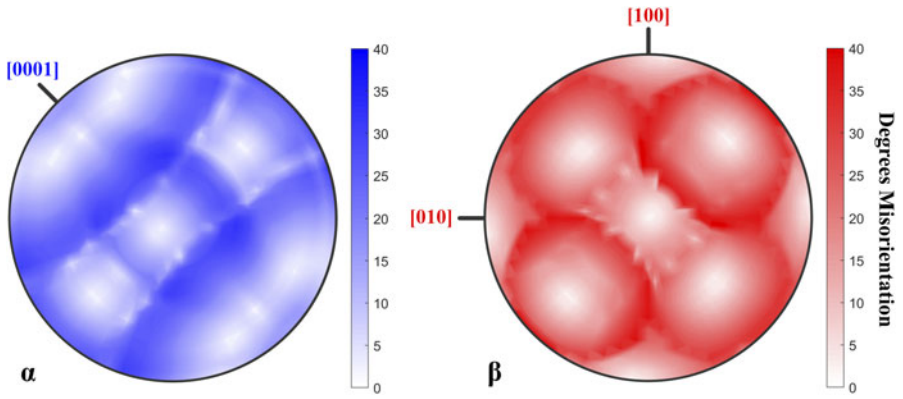

Figure 3: Misorientation of the α and β phases at a strain of 1.0 relative to their initial orientations.

misorientation angles, primarily present for loading along the ⟨*a*⟩ directions of the α phase, could correspond to either corotation or initially stable orientations.

The misorientation of each phase relative to its initial orientation was used to distinguish between loading directions undergoing corotation versus stable orientations. These changes in orientation of the individual α and β phases during loading is illustrated in Fig. 3 at the final strain increment. Animated GIFs of the evolution with strain are available in Supplementary material Figs. S3 and S4. For the β phase, stable orientations corresponded to loading along ⟨001⟩ or ⟨111⟩ directions. For the α phase, stable orientations were loading along the $\langle 11\bar{2}0\rangle$ or at angles of approximately 15° from the *c* axis.

The relationship between the single-phase misorientation plots and the BOR deviation plot is clear; the low misorientation "band" in Fig. 2 corresponds to the coincidence of the ⟨*a*⟩ directions in the basal plane with the β slip directions in the (110) plane.

Cross-referencing Figs. 2 and 3 allows for classification of each loading direction into the categories of corotation, antirotation, or stable orientation, as shown in Fig. 4. As a preliminary binning strategy, a threshold of 20° was used as the cutoff for "high" misorientation. The selection of an appropriate threshold is further discussed below. Using conditional comparisons of the misorientation matrices, Fig. 4 plots how regions of orientation space correspond to the three hypothesized conditions. Under this assumed threshold, corotation is relatively uncommon but does occur, whereas antirotation or stable orientations dominate. This suggests that cooperative rotation of α and β to maintain the BOR is a minor factor in the persistence of lamellar colonies through deformation processing. Instead, the grains either rotate apart or simply do not experience significant rotation during plastic deformation.

In reality, the selection of the threshold is more qualitative than quantitative. A physically based estimate of a threshold would be 10–15°, as that is a misorientation corresponding to the formation of a "high angle grain boundary." However, VPSC simulations are notorious for overpredicting the intensity of deformation textures even when the texture is qualitatively correct [16, 17, 18, 19, 20, 21, 22, 23]. Because

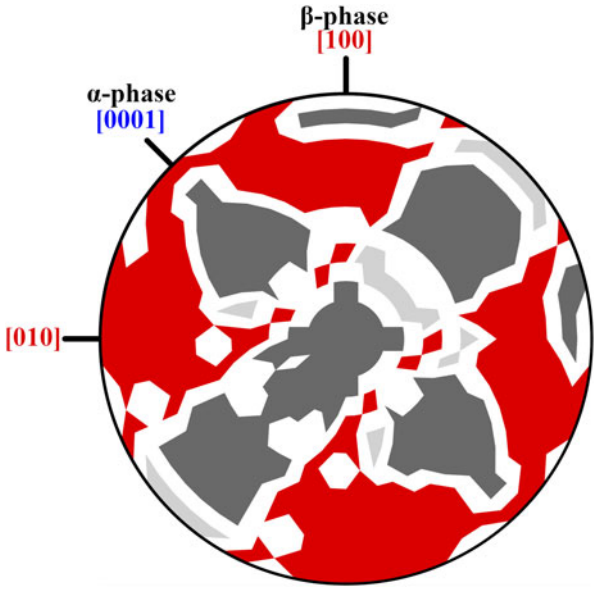

Figure 4: Binning of loading orientations into corotation (light gray), initially stable orientations (dark gray) or antirotation (red) using a threshold of 20°. White areas are indeterminate under this binning strategy.

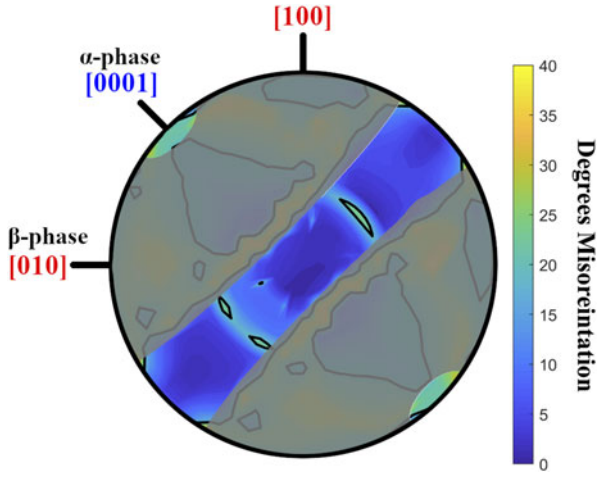

Figure 5: Results from Bieler and Semiatin superimposed on the results from Fig. 2. Unaltered regions were observed to have sluggish globularization kinetics.

of this known behavior, the authors selected a higher initial threshold guess of 20°. Calibration and refinement of the thresholding conditions require comparison to experiment.

The most relevant experimental work in the literature is that of Bieler and Semiatin [24], who used electron backscatter diffraction (EBSD) to study the effect of axisymmetric compression on globularization of Ti–6Al–4V alloy containing colonies of approximately 100 μm inside of 400 μm prior beta grains. Specifically, they considered the dependence of globularization on colony orientation. Notably, the number of studied colonies was small due to the speed limitations of EBSD at the time of the work. This produces limited fidelity in orientation space. Nonetheless, they found that the rate of globularization is inhibited when the *c* axis of the α phase is less than 15° or greater than 75° from the loading direction.

This condition is overlaid on the plot of deviation from initial BOR in Fig. 5, where the loading directions without an overlay were observed to have sluggish globularization kinetics. Loading directions lying near or in the basal plane show excellent agreement between the experimental observations and the VPSC simulations. This comparison suggests that the 20° threshold is appropriate, although further data collection may lead to refinement. An animated GIF showing binning as a function of the threshold is presented in the Supplementary material Fig. S5.

Careful consideration is necessary when discussing grains whose *c*-axis is nearly parallel to the loading direction. In the VPSC simulations, these loading directions predict moderate antirotation, suggesting no issues with globularization. However, this is not what has been experimentally observed. These hard orientations often undergo kinking (buckling), leading to nonuniform globularization behavior. The buckled segments tend to rapidly globularize, while the remaining segments of hard orientation remain lamellar and resist globularization [24]. This is in apparent contrast to the VPSC results presented herein.

However, loading aligned with the *c*-axis is a hard orientation; in real multicolony specimens, other colonies would preferentially deform. The effective strain in colonies of hard orientations would be lower, and buckling is not possible in the remaining short segments. If single-colony compression were carried out to large strains for hard orientations to achieve the nominal strains (without buckling), globularization would be predicted, but this is not physical for typical Ti processing. Because of these issues, VPSC simulations using stress control may have more predictive power for polycolony specimens than those using strain control. Further experimental work on hard colonies is necessary for more direct experimental comparison.

Bieler and Semiatin also drew conclusions about the contribution of slip system activity to lamellar breakdown. They attributed the enhanced rate of lamellar breakdown in the 15°–75° range around the *c* axis to the combination of basal and prismatic slip systems acting synergistically to facilitate globularization.

This combined slip criterion can be compared to the slip system activities predicted by the VPSC model, as illustrated in Fig. 6. As shown in subfigures, Figs. 6(a) and 6(b), loading near parallel to the *c*-axis does result in both low basal slip activity and low prismatic slip activity; this is strongly in agreement with Bieler and Semiatin for these orientations. The subfigure Fig. 6(c) illustrates the reliance on pyramidal $\langle c + a \rangle$ slip for these loading directions.

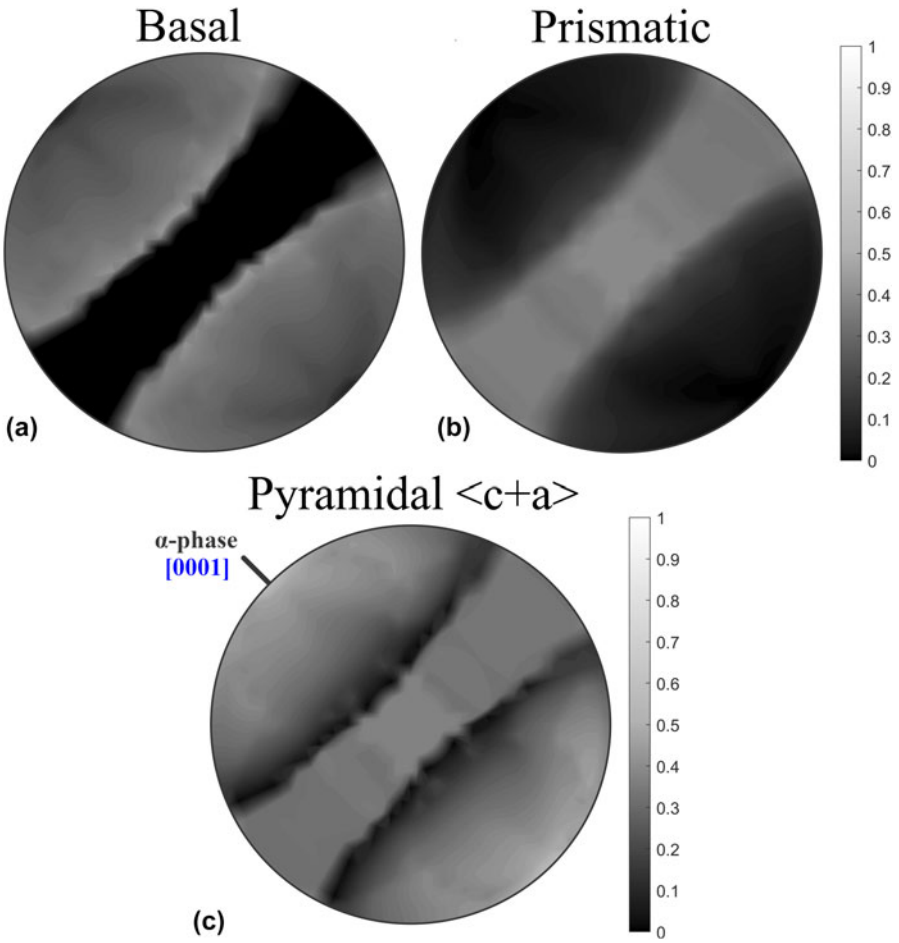

Figure 6: VPSC predicted (a) basal, (b) prismatic, and (c) pyramidal slip activity as a function of loading direction. Presented on a scale normalized to total slip system activity from 0 (dark) to 1 (white).

Further insight into the relationship between total slip activity and the resulting crystal rotations can be gained by looking at the axes about which rotation between the initial and final orientations is occurring, particularly within the α phase (Figs. 7 and S6). These rotation axes can be compared with the Taylor axes for different slip families. For the α phase, many rotations appear in red, corresponding to rotation around the *c* axis caused by primarily prismatic slip. Under these near single-slip conditions, it would be possible to undergo recovery instead of recrystallization and lamellar breakdown. Other loading directions that accumulate significant misorientation are clearly in multiple slip orientations.

Extended globularization criteria including both slip and crystal rotation are proposed. It is suggested that both antirotation of the two phases and combined activity of basal and prismatic slip are necessary for globularization. This set of combined criteria can be justified from a microstructural perspective, as discussed below.

Bieler and Semiatin state that the activity of both basal and prismatic slip is necessary to "slice" the lamella into smaller pieces via slip transmission. Slip transmission through the α–β interface has been observed for both basal and prismatic slip [25]. However, the present results suggest that slip transmission is not the sole reason for the importance of combined basal and prismatic slip, because the present model would not capture transmission behavior. Additionally, if slip transmission was the defining factor, the activity of $\langle a1 \rangle$ and $\langle a2 \rangle$ slip would be predicted to be the most important, as these are the Burgers vectors with the lowest misalignment across the BOR interface (and therefore the most likely to undergo slip transmission). Instead, the summation of all three $\langle a \rangle$ Burgers vectors has the most predictive power.

Rather than slip transmission, the contribution of multiple basal and prismatic slip systems is likely related to recrystallization criteria which have been discussed in other hcp alloys, most notably Mg. In Mg alloys, grains where multiple Burgers vectors are active recrystallize more readily. This is because the formation of a high angle boundaries is dependent on the synergistic activity of multiple basal and prismatic slip families to rotate the subgrain away from the parent [26, 27, 28].

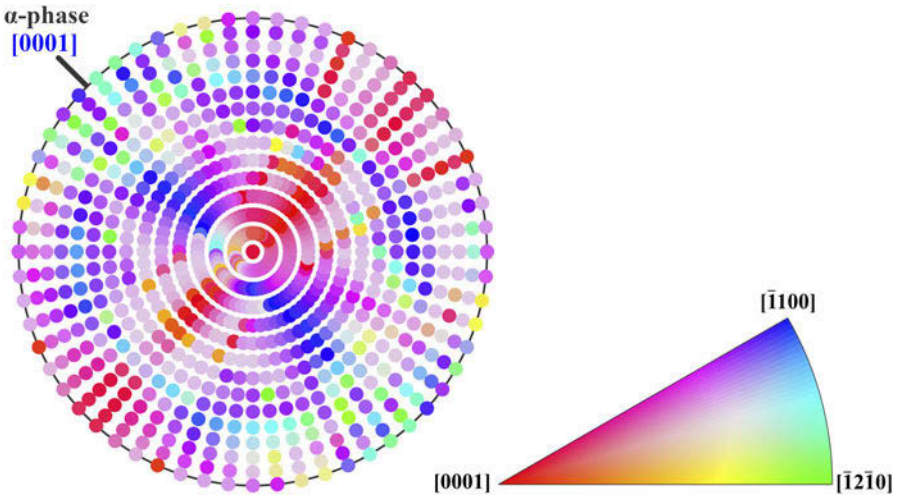

Figure 7: α phase misorientation axes at a strain of 1.0 relative to the initial orientation.

Based on the results of this work, for lamellar α–β Ti colonies, antirotation of the two phases is necessary to promote breakdown of the BOR. Additionally, synergistic activity of basal and prismatic slip in the α phase is necessary to promote the formation of smaller equiaxed α grains and potentially to break up the β phase lamella.

In summary, the results of our VPSC model agree well with the existing empirical work studying the mechanisms of lamellar breakdown in α + β titanium alloys. Our model agrees with the experimental observation that basal and prism slip work cooperatively to facilitate globularization and provides insight into the loading orientation dependence of slip system activity. The results of this model also suggest that there is substantially more to the orientation dependence of globularization than the previously reported basal pole tilt criteria. Of particular interest would be basal pole tilts of approximately 45° where there is a range of predicted globularization behavior. This is a potential avenue for further experimental study.

Summary and conclusions

In this work, the VPSC polycrystal plasticity model was used to predict deformation behavior of α + β colonies as a function of loading direction. It was demonstrated that the colony crystal rotation behavior can be classified into "corotation" where both phases undergo similar rotations, "antirotation" in which the phases rotate apart, or minimal rotation when the initial orientation was stable for both phases. However, this alone was demonstrated to be an insufficient criterion to predict globularization. Orientations that have been reported to undergo globularization readily must both (i) undergo significant antirotation during deformation and (ii) have substantial amounts of both basal and prismatic slip.

These findings illustrate that globularization behavior in two-phase Ti alloys can be predicted with substantial accuracy using computationally inexpensive mean-field polycrystal plasticity methods. Additionally, it suggests that there is additional detail to the orientation dependence of globularization kinetics that has not previously been reported based on experimental results; however, further investigation is required.

Methods

The α–β Ti system was simulated using a VPSC model to observe the rotation and corotation of the grains. This framework considers each grain as an Eshelby inclusion in a homogeneous effective medium with the elastic properties of the aggregate polycrystal [29]. A macroscopic deformation is imposed, and shear rates are calculated on the relevant slip systems for each grain. These shear rates are used to calculate crystallographic texture evolution, grain-scale hardening, slip activity, and macroscopic stress–strain behavior. All simulated mechanical tests in this work are uniaxial compression tests along a specified direction relative to the colony orientation at a strain rate of 10^{-2} s^{-1}. Results were not found to be strongly sensitive to the deformation rate.

The VPSC model typically uses an extended Voce law to describe the hardening behavior of each slip system. The necessary parameters to model this behavior accurately for α + β alloys are absent in the existing literature, so in this case each system is assumed to be perfectly plastic. The τ_0 (effective CRSS) values determined experimentally by Salem and Semiatin, given in Table I, were assigned in the model [30].

Nine hundred fifteen axisymmetric uniaxial compression directions were simulated, uniformly sampling one hemisphere of orientation space to eliminate redundancy from the loading symmetry associated with uniaxial tests. The BOR has

TABLE I: Effective critical resolved shear stress values for each slip system in a single α–β Ti colony, from Ref. 30.

Slip system	τ_0 (MPa)
a_1 basal	73
a_2 basal	61
a_3 basal	54
a_1 prismatic	43
a_2 prismatic	61
a_3 prismatic	81
$\langle c + a \rangle$ pyramidal	119

monoclinic crystal symmetry [31], which is reflected in the results presented above. Small deviations from perfect monoclinic symmetry result from rounding errors. For numerical stability, 200 identically oriented grains of each phase were simulated; the VPSC results are deterministic, so this results in only a single α and β orientation for each loading condition. Equal angle projections are used in this work to plot rotation and misorientation results in orientation space. The β phase was chosen as the origin orientation, rotating through the BOR Euler angles to establish the initial alpha orientation [3]. These figures are therefore relative to the ⟨001⟩ axis of the cubic β phase. Angular deviation from the initial orientation relationship is used to represent misorientations.

Deformation was simulated to a compressive strain of 1.0, with the texture being updated at strain increments of 0.05. The MTEX toolbox [32] was used to import the starting and as-deformed orientations, along with slip system activities, for further analysis. Strain evolution of misorientation and slip activity were captured by generating multiframe image files, accessible through online Supplemental material.

The code used to analyze the simulation data has been published at https://github.com/tori-miller/Ti64-VPSC-CoRotation-Analysis.

Supplementary material

To view supplementary material for this article, please visit https://doi.org/10.1557/jmr.2020.54.

References

1. **S.L. Semiatin, V. Seetharaman, and I. Weiss**: The thermomechanical processing of alpha/beta titanium alloys. *JOM* **49**, 33–39 (1997).
2. **W.G. Burgers**: On the process of transition of the cubic-body-centered modification into the hexagonal-close-packed modification of zirconium. *Physica* **1**, 561–586 (1934).
3. **U. Dahmen**: Orientation relationships in precipitation systems. *Acta Metall.* **30**, 63–73 (1982).
4. **D. Banerjee and J.C. Williams**: Perspectives on titanium science and technology. *Acta Mater.* **61**, 844–879 (2013).
5. **I. Weiss and S.L. Semiatin**: Thermomechanical processing of alpha titanium alloys—An overview. *Mater. Sci. Eng., A* **263**, 243–256 (1999).
6. **N. Stefansson and S.L. Semiatin**: Mechanisms of globularization of Ti–6Al–4V during static heat treatment. *Metall. Mater. Trans. A* **34**, 691–698 (2003).
7. **N. Stefansson, S.L. Semiatin, and D. Eylon**: The kinetics of static globularization of Ti–6Al–4V. *Metall. Mater. Trans. A* **33**, 3527–3534 (2002).
8. **R.M. Poths, B.P. Wynne, W.M. Rainforth, J.H. Beynon, G. Angella, and S.L. Semiatin**: Effect of strain reversal on the dynamic spheroidization of Ti–6Al–4V during hot deformation. *Metall. Mater. Trans. A* **35**, 2993–3001 (2004).
9. **M. Peters, G. Lütjering, and G. Ziegler**: Control of microstructures of (alpha + beta)-titanium alloys. *Z. Met.* **74**, 274–282 (1983).
10. **S.L. Semiatin and D.U. Furrer**: Modeling of microstructure evolution during the thermomechanical processing of titanium alloys. *ASM Handb.* **22**, 522–535 (2009).
11. **S. Mironov, M. Murzinova, S. Zherebtsov, G.A. Salishchev, and S.L. Semiatin**: Microstructure evolution during warm working of Ti–6Al–4V with a colony-α microstructure. *Acta Mater.* **57**, 2470–2481 (2009).
12. **I. Weiss, F.H. Froes, D. Eylon, and G.E. Welsch**: Modification of alpha morphology in Ti–6Al–4V by thermomechanical processing. *Metall. Trans. A* **17**, 1935–1947 (1986).
13. **S.L. Semiatin, N. Stefansson, and R.D. Doherty**: Prediction of the kinetics of static globularization of Ti–6Al–4V. *Metall. Mater. Trans. A* **36**, 1372–1376 (2005).
14. **C.H. Park, J.W. Won, J-W. Park, S.L. Semiatin, and C.S. Lee**: Mechanisms and kinetics of static spheroidization of hot-worked Ti–6Al–2Sn–4Zr–2Mo–0.1Si with a lamellar microstructure. *Metall. Mater. Trans. A* **43**, 977–985 (2012).
15. **L. Germain, N. Gey, M. Humbert, P. Bocher, and M. Jahazi**: Analysis of sharp microtexture heterogeneities in a bimodal IMI 834 billet. *Acta Mater.* **53**, 3535–3543 (2005).
16. **V.M. Miller, T.D. Berman, I.J. Beyerlein, and T.M. Pollock**: Prediction of formability in magnesium alloys: The role of texture. In *Magnesium Technology 2016, TMS*, Edited by Alok Singh, Kiran Solanki, Michele V. Manuel, and Neale R. Neelameggham. (The Minerals, Metals & Materials Society, Nashville, TN, 2016); pp. 257–262.
17. **V.M. Miller, T.D. Berman, I.J. Beyerlein, J.W. Jones, and T.M. Pollock**: Prediction of the plastic anisotropy of magnesium alloys with synthetic textures and implications for the effect of texture on formability. *Mater. Sci. Eng., A* **675**, 345–360 (2016).
18. **V.M. Miller, S.L. Semiatin, C. Szczepanski, and A.L. Pilchak**: Optimization of VPSC model parameters for two-phase titanium alloys: Flow stress Vs orientation distribution function metrics. *Metall. Mater. Trans. A* **49**, 3624–3636 (2018).
19. **S.C. Vogel, I.J. Beyerlein, M.A. Bourke, C.N. Tomé, P. Rangaswamy, C. Xu, and T.G. Langdon**: Texture in equal-

channel angular pressed aluminum and nickel. *Mater. Sci. Forum* **408–412**, 673–678 (2002).

20. **S.G. Vogel, D.J. Alexander, I.J. Beyerlein, M.A. Bourke, D.W. Brown, B. Clausen, C.N. Tomé, B.R. Von Dreele, C. Xu, and T.G. Langdon**: Investigation of texture in ECAP materials using neutron diffraction. *Mater. Sci. Forum* **426–432**, 2661–2665 (2003).
21. **J.S. Carpenter, R.J. McCabe, S.J. Zheng, T.A. Wynn, N.A. Mara, and I.J. Beyerlein**: Processing parameter influence on texture and microstructural evolution in Cu–Nb multilayer composites fabricated via accumulative roll bonding. *Metall. Mater. Trans. A* **45**, 2192–2208 (2014).
22. **S. Li, I.J. Beyerlein, D.J. Alexander, and S.C. Vogel**: Texture evolution during multi-pass equal channel angular extrusion of copper: Neutron diffraction characterization and polycrystal modeling. *Acta Mater.* **53**, 2111–2125 (2005).
23. **S. Li, I.J. Beyerlein, C.T. Necker, D.J. Alexander, and M. Bourke**: Heterogeneity of deformation texture in equal channel angular extrusion of copper. *Acta Mater.* **52**, 4859–4875 (2004).
24. **T.R. Bieler and S.L. Semiatin**: The origins of heterogeneous deformation during primary hot working of Ti–6Al–4V. *Int. J. Plast.* **18**, 1165–1189 (2002).
25. **M.P. Echlin, J.C. Stinville, V.M. Miller, W.C. Lenthe, and T.M. Pollock**: Incipient slip and long range plastic strain localization in microtextured Ti–6Al–4V titanium. *Acta Mater.* **114**, 164–175 (2016).
26. **J.P. Hadorn, K. Hantzsche, S. Yi, J. Bohlen, D. Letzig, J.A. Wollmershauser, and S.R. Agnew**: Role of solute in the texture modification during hot deformation of Mg-rare earth alloys. *Metall. Mater. Trans. A* **43**, 1347–1362 (2011).
27. **J.P. Hadorn, K. Hantzsche, S. Yi, J. Bohlen, D. Letzig, and S.R. Agnew**: Effects of solute and second-phase particles on the texture of Nd-containing Mg alloys. *Metall. Mater. Trans. A* **43**, 1363–1375 (2012).
28. **V.M. Miller and T.M. Pollock**: Texture modification in a magnesium–aluminum–calcium alloy during uniaxial compression. *Metall. Mater. Trans. A* **47**, 1854–1864 (2016).
29. **R.A. Lebensohn and C.N. Tomé**: A self-consistent anisotropic approach for the simulation of plastic deformation and texture development of polycrystals: Application to zirconium alloys. *Acta Metall. Mater.* **41**, 2611–2624 (1993).
30. **A.A. Salem and S.L. Semiatin**: Anisotropy of the hot plastic deformation of Ti–6Al–4V single-colony samples. *Mater. Sci. Eng., A* **508**, 114–120 (2009).
31. **J-Y. Kim and S.I. Rokhlin**: Determination of elastic constants of generally anisotropic inclined lamellar structure using line-focus acoustic microscopy. *J. Acoust. Soc. Am.* **126**, 2998–3007 (2009).
32. **F. Bachmann, R. Hielscher, and H. Schaeben**: Texture analysis with MTEX—Free and open source software toolbox. *Solid State Phenom.* **160**, 63–68 (2010).